Numerical analysis of the onset of the vapor-liquid phase in a single horizontal low carbon steel water tube.

Jarryd Wyngaard, Thokozane Kunene, Lagouge Tartibu
Faculty of Engineering and Built Environment (FEBE)
University of Johannesburg
Auckland Park, JHB, PO Box 524, RSA
jarrydwyngaard@gmail.com, tkunene@uj.ac.za, ltartibu@uj.ac.za

Abstract

Boiler tube failures occur in steam generation boilers due to subcritical Short Term Overheating (STO). In general, sub-critical STO occurs when design parameters are often marginally and critically discounted. This leads to frequent failures of the boiler tubes that affect the sustainability of power generation. A commercial Computational Fluid Dynamics (CFD) software, ANSYS Fluent 19.0® (Multiphase flow), was used to successfully analyze the locations where the phase boundary of energy transfer on the tube material occurs. A number of heat transfer velocity parameter changes were numerically analyzed to determine the integrity operating window in which the tube could perform, with further analysis done to predict the useful life when operating in this sub-critical STO zone. Numerical analysis is limited to a horizontal carbon steel water tube of 36.6mm ID operating at 17.6MPa with a uniform heat flux.

Keywords

Computational Fluid Dynamics
Power Generation Boilers
Horizontal Tube
Multiphase Flow
Heat Transfer

1. Introduction

Tube failures occur in new and old units; in units that cycle and those that operate under baseload conditions; in supercritical, once-through, and drum units; and in units burning every sort of combustible material (Martin, 2009).
In conventional and combined-cycle plants, boiler tube failures (BTFs) have been the main cause of plants unavailability for as long as reliable statistics have been kept for each generating source. Tube failures emanate from poor initial design, poor operation and maintenance, harsh fireside and cycle chemistry environments, and lack of management support for comprehensive reduction programs. Most BTFs are repeat failures, indicating that return to service of a unit has historically been more important than understanding the failure (Martin, 2009).

If there are no breakdowns from the original design conditions, water-touched tubes (such as waterwalls and economizers in conventional boilers) are designed for, and should have, essentially infinite life. The case for steam-touched tubes, such as in the superheater (SH) and reheater (RH) sections of modern boilers, is somewhat different because of the inevitability of creep-limited lifetime, although lifetimes well in excess of 200,000 operating hours are achievable (Dooly & McNaughton, 2007).

In almost all cases of serious unavailability or performance losses, the problems are usually repetitive in nature and result in multiple forced outages. A repeat tube failure is defined as multiple failures in the same boiler circuit from the same mechanism and root cause. Without a proper understanding of the mechanism of failure, the root cause, the

appropriate corrective actions, and the proper execution of those actions, it is not possible to implement suitable corrective engineering approaches.

Short term overheating in water-cooled tubes occurs because of abnormal coolant flow or excessive combustion gas temperature. As a result, the tube is subjected to excessively high temperature, often hundreds of degrees above design, which results in rapid failure (Dooley & McNaughton, 2007).

Pronounced microstructural changes are evident in this type of failure; those changes can be used as a diagnostic to estimate the tube temperature reached at burst (French, 1993).

Three levels of "short term" overheating have been classified, depending on whether the temperature at burst was (i) below the lower critical temperature, A1, (termed "subcritical short term overheating"), (ii) between A1 and A3 - the upper critical temperature (termed "intercritical short term overheating"), or above A3 (termed "upper critical short term overheating") (Dooley & McNaughton, 2007) (Figure 1. Equilibrium Diagram for Iron-Iron Carbide)

Pronounced local bulging occurs because of the decrease in strength of the tube metal. The level of overheating (subcritical, intercritical, or upper critical) will depend on the temperature reached by the tube and the length of time of the transient or operating feature that underlies the problem (Dooley & McNaughton, 2007).

The root causes for Short-Term overheating of waterwall tubes has been identified by the Electric Power Research Institute to be partial blockages caused by maintenance activities, plugging of waterwall orifices by corrosion products, formation of nodule deposits within the system, poor drum level control, loss of coolant due to an upstream failure.
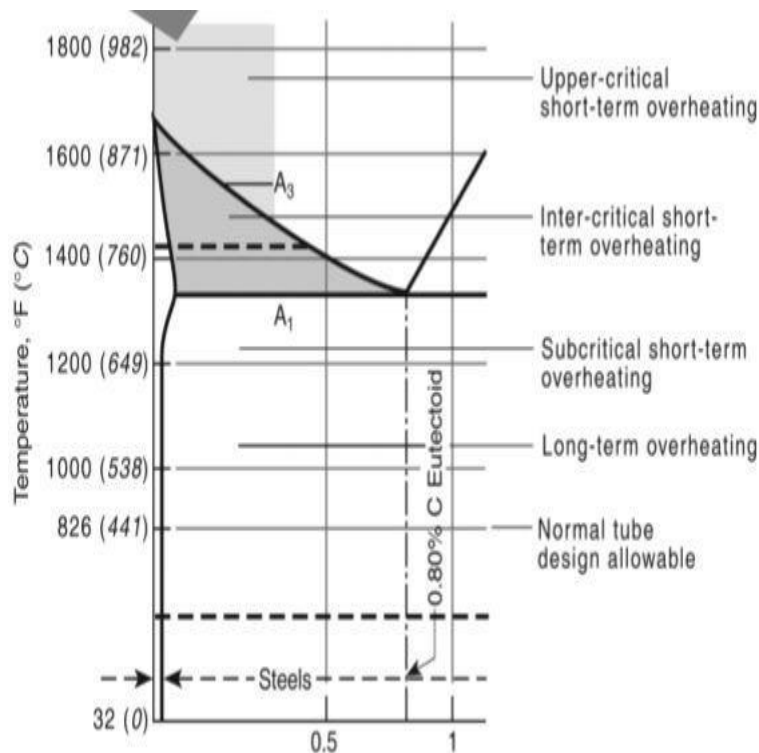

Figure 1. Equilibrium Diagram for Iron – Iron Carbide (Dooley, 2007:34-2)

Flow patterns formed during the generation of vapor in horizontal evaporator tubes are shown in Figure 2. Flow Patterns in Horizontal Evaporator Tubes, (Collier & Thome, 1994).

The schematic representation of a horizontal tubular channel heated by a uniform low heat flux and fed with liquid just below the saturation temperature for a relatively low inlet velocity illustrates the sequence of flow patterns which might be observed. Asymmetric distributions of the vapor and liquid phases due to the effects of gravity introduce new complications compared to vertical up-flow. Important points to note from a heat transfer standpoint are the possibility of complete drying or intermittent drying of the tube wall around part of the tube perimeter, particularly in slug and wavy flow and for annular flow with partial dry-out. For example, in annular flow the film is thicker in the bottom than at the top and progressively increases around the perimeter of the tube in the direction of flow. In wavy flow, the top of the tube may be intermittently dry if the waves wash the top of the tube or always dry if they do not. These waves leave behind thin films of liquid that may not evaporate completely before the arrival of the next wave (Thome, 2007:10-16).
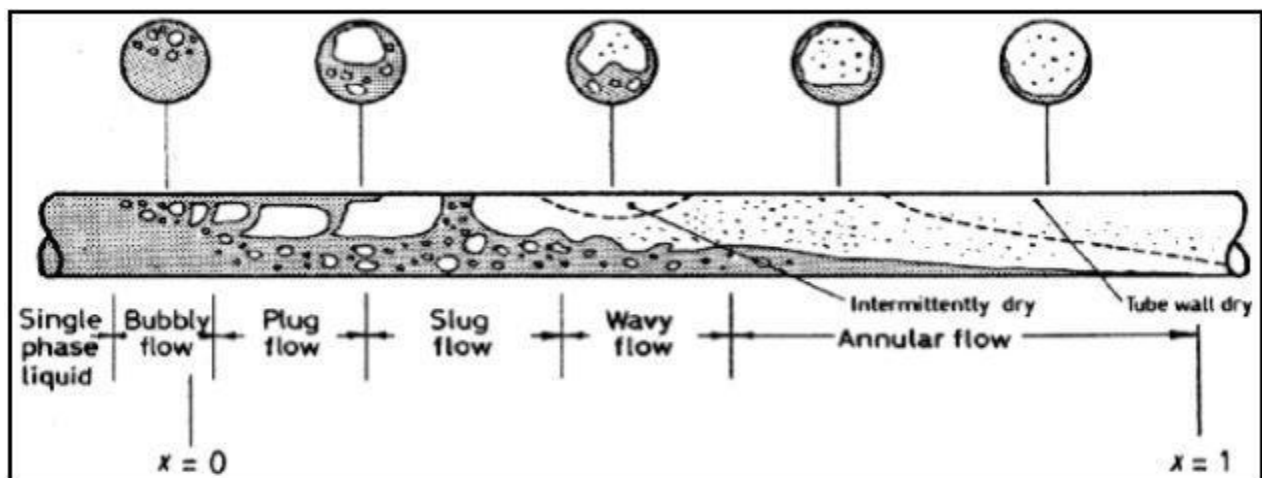

Figure 2. Flow Patterns in Horizontal Evaporator Tubes (Collier & Thome, 1994)

If the heat flux of a boiling system is higher than the critical heat flux (CHF) of the system, the bulk fluid may boil, or in some cases, regions of the bulk fluid may boil where the fluid travels in small channels. Thus large bubbles form, sometimes blocking the passage of the fluid. This results in a departure from nucleate boiling (DNB) in which steam bubbles no longer break away from the solid surface of the channel, bubbles dominate the channel or surface, and the heat flux dramatically decreases. Vapor essentially insulates the bulk liquid from the hot surface.

During DNB, the surface temperature must therefore increase substantially above the bulk fluid temperature in order to maintain a high heat flux. DNB is also known as Transition boiling, unstable film boiling, and partial film boiling. For water boiling as shown in Figure 2, transition boiling occurs when the temperature difference between the surface and the boiling water is approximately 30°C to 120°C above the Ts. This corresponds to the high peak and the low peak on the boiling curve graph.

During transition boiling of water, the bubble formation is so rapid that a vapor film or blanket begins to form at the surface. However, at any point on the surface, the conditions may oscillate between film and nucleate boiling, but the fraction of the total surface covered by the film increases with increasing temperature difference. As the thermal conductivity of the vapor is much less than that of the liquid, the convective heat transfer coefficient and the heat flux reduces with increasing temperature difference (Bergman, et al., 2011).

The distribution of individual fluid phases describe the configuration of the flow pattern of a multiphase flow which is being determined by the interaction of gravity, surface tension, evaporation, inertia, shear and bubble nucleation forces in liquid-vapor interface (Karayiannis, 2010).

The understanding of the flow patterns is crucial; it affects design parameters and determines the heat transfer coefficient, critical heat flux and pressure drop in a system (Tibirica, 2013).

Stratified or churn flow pattern is observed in a macro-channel during two-phase flow in evaporators at lower total mass fluxes. As the diameter reduces in horizontal channel, gravitational effects become negligible, while the inertia force becomes significant to form annular flow pattern. Heat flux also becomes more significant in two-phase flow pattern at microscale. (Kandlikar, 2010)

LiLi et al (2012) performed numerical analysis of the flow and boiling heat transfer of two phases within horizontal tubes, and concluded that velocity increase, increased the drag force of generated bubbles and increased the heat transfer coefficient. Their post-processing indicated how the generated vapor tended to move to the upper periphery of the tube, with an increase in tube temperature in the upper region being noted.

Ekambara, K et al (2008) numerically analyzed a 50.3mm ID horizontal tube with flow velocities varying between 3.8 – 5.1 m/s and 0.2 – 1.0 m/s with the aid of a multiphase model, and their results deduced that volume fraction has a maximum near the upper pipe wall, and the profiles tend to flatten with increasing liquid flow rate. The axial liquid mean velocity showed a relatively uniform distribution except near the upper pipe wall. An interesting feature of the liquid velocity distribution is that it tends to form a fully developed turbulent pipe-flow profile at the lower part of the pipe irrespective of the liquid and gas superficial velocities.

In the paper, Prediction of Risers' Tubes Temperature in Water Tube Boilers by Emara-Shabaik et al (2009), a dynamic model is developed to prevent boiler tube overheating. This model gives a detailed account of the two-phase heat transfer process which takes place between the risers' inner wall and the water-steam mixture flow inside the tube. The experiments are limited to vertical tubes and the model specifically looks at start-up conditions where boiler operations undergo step transient periods with rapid rises in heat flux and tube internal flow velocities.

Yu et al (2013) conducted experiments in horizontal tubes with inner diameters of 26 mm and 43 mm. Operating conditions included mass fluxes of 300–1000 kg/m2 s, heat fluxes up to 400 kW/m2, and a pressure of 25 MPa. It was found that the buoyancy effect makes the low density hot water gather at the top surface of the horizontal tube; hence, heat transfer condition is deteriorated and wall temperature is increased.

Recent literature indicates analysis being performed predominantly on micro-channels with the working fluids being refrigerants or nano-fluids.

da Silva Lima, R.J et al (2009) presented experimental studies with flow boiling heat transfer results of R-134a flowing inside a 13.84 mm internal diameter, smooth horizontal copper tube. The experimental results clearly show that a local minimum heat transfer coefficient systematically occurs within slug flow pattern or near the slug-to-intermittent flow pattern transition. For slug flow, methods that require the identification of nucleate boiling related regions tend to predict the heat transfer coefficient accurately. This emphasizes that for slug flows, heat transfer is not a simple juxtaposition of nucleate and convective boiling contributions, but that the integration of these two heat transfer mechanisms is also a function of flow parameters. Their comparisons between experimental and predicted data show that the best overall results are obtained with superposition and flow pattern based methods.

Moss et al (2000) performed studies on two types of boilers at Mobil's Altona Refinery which had been operating for over 20 years. Their key intention was to determine remaining life calculations based on the possibility of accelerated creep. However, going from creep rupture test results to assess the remaining life of furnace tubing is complicated by the fact that the tested tubes may not have been exposed to the maximum temperature for the life of the furnace the test stress is different from the service stress because various pressure and wall thickness combinations exist. To overcome such issues detailed heat transfer calculations were carried out to understand tube temperatures based on thermography data and assessment of consumed life fraction was undertaken. Deterministic modelling of total life based on wall thickness data and operating pressure was carried out using the most appropriate creep rupture database. Their studies indicated that operating temperature limits were required to ensure that the boilers could run safely to their next planned tube replacement outages.

The water wall tubes run in a hazardous environment, and the fire, gas and coal ash often attack the tube and corrosion, erosion and fatigue cause the tube wall thickness decrease and fail, and can even lead to explosion and leakage, by which the safety and cost-effectiveness of the thermal power plant is seriously influenced. The explosion and leakage of boiler tubes in power plants is a serious problem that often leads to unscheduled and costly outages. (Xuequin, L et

al, 2008). Waterwall tube failures result in the furnace pressure becoming positive and thus pressurized water and steam, as well as combustion products are expelled through the furnace observation windows and doors. If a sudden high pressure release is realized, the rapid increase in furnace pressure could result in rupture of the containment walls and damage to the boiler structure which could significantly affect the safety of personnel.

Ray et al (2000) performed residual life assessments and safety assessments on service-exposed thermal power boiler waterwall tubes by doing destructive as well as non-destructive tests. Their results showed that high levels of safety risk could easily be minimized or completely mitigated if operating limits were adhered to.

In the paper "Study for Accident of Steam Boiler Tube Burst" by Wei L et al (2008), foundations were set for the prevention of steam boiler tube burst failures. Comparison of the components' macroscopic and microscopic morphology indicated the major cause of the boiler tube burst to be excessively high wall temperatures under operational conditions.

2. Motivation

The reason for performing this numerical analysis is to determine the integrity operating window in which a specific sized boiler carbon steel tube may operate. This rationale is determined from repeat failures occurring in Eskom's Arnot Power Station Boiler 3. The fault-finding processes of the Electric Power Research Institute have been greatly exhausted, with no direct cause for the repeat failures being identified.

The Authors of this paper have directed their numerical simulations around the developed flow map regimes under changing flow velocities, with constant wall temperature flux. It is of their interest, to evaluate how the developed flow map changes with an increase in fluid velocity. This can then be directly related to future modifications of tube flow throttling and condition monitoring to prevent the onset of the sub-critical STO. By changing the velocity, it indirectly simulates operating conditions where partial flow disruptions are occurring within the system, as well as operating regimes where the heat input might be excessive for the generated boiler load which is determined by the fluid flowrate.

Current experiments (LiLi et al. 2012) have been performed around the studies of wall temperature and fluid flow changes to enhance the heat transfer characteristics of the fluid flow, with no direct relation being instituted to the effects it has on the fluid containment material. Velocity changes have also been minor, and thus would not indicate maximum allowable velocities, under which linear heat transfer changes within the fluid no longer occurs.

By performing the numerical analysis, profiles can be developed for low-carbon steel boiler tubes to better predict the remaining useful life when operated at above-design parameters, as well as determine maximum heat transfer positions relative to tube length based on the internal flow and heat flux conditions. Comparisons can be made as to the flow maps based on published studies.

3. Methodology

Demineralized water was considered as the working fluid for the generation of the three-dimensional, unsteady, vapor-liquid two-phase numerical model. A low carbon steel tube (BS3059.440) of 1m length and 36.6mm internal diameter was considered. Using Autodesk Inventor ® to model the tube geometry, the 3D model was transferred to a student version of ANSYS Fluent 19.0® (Multiphase flow). The following simulation was run over a distance of 400mm and all discussions and conclusions based on this domain length.

The Fluent multiphase flow model was selected for the numerical analysis. In this simulation of the vapor-liquid two-phase flow the mixture model utilizes the energy, momentum and continuity conservation equations. It also requires the slip velocity and volume fraction equations.

The algebraic expression for relative speed is given as:

$$\vec{v}_{pq} = \frac{\tau_p}{f_{drag}} \frac{(\rho_p - \rho_m)\vec{a}}{\rho_p}$$

Where the vector of $\vec{a}$ is acceleration, f_{drag} is the drag coefficient in the application of Fluent, and τ_p is the relaxation time of the particle.

The volume fraction equation is used for the calculation of different phase's share of the space volume, and given as:

$$\frac{\partial}{\partial_t}(\alpha_p \rho_p) + \nabla.(\alpha_p \rho_p \vec{v}_m) = -\nabla.(\alpha_p \rho_p \vec{v}_{drp}) + \sum_{q=1}^{n}(m_{qp}^0 - m_{pq}^0)$$

Where m_{qp}, m_{pq} is the interaction quality transformation source item between vapor and liquid.

Inlet boundary: The inlet boundary has selected conditions of velocities being 10m/s, 5m/s and 3m/s with the inlet temperature being 671K and turbulence intensity of 5%. The inlet pressure parameter is 17.6MPa. Exit boundary had zero gauge pressure. Wall condition had no slip wall condition for the low-carbon steel tube and the temperatures taken as 380 w/m^2.

In the 3D implicit separation solver, the pressure-speed coupling was set as SIMPLE, and the discretization of the pressure equation set as Standard. The momentum, energy and volume fraction equations were discretized by the first order. The set residual criteria during the simulation runs were set as follows: energy = x10^{-6} continuity = x10^{-9} and speed = x10^{-6}

The effect of grid density was analyzed to verify grid element size independence. The meshing begins with the default size (Global meshing) of the tetrahedral elements used in order to discretize the model configuration as imposed by ANSYS Fluent 19.0. The grid size was reduced subsequently and the effect of the resulting change on the skin friction coefficient of the pipe wall was calculated. The skin friction coefficient was calculated relative to grid size as seen in Table 2. It shows that the calculated static pressure at the outlet of the pipe has very small changes less than 0.02% until a max face size of 2.5mm with 378692 elements was reached.

Table 1. Grid-Independent Data

Skin friction Coeff. (-)	Elements (-)	Max., Face. Size (mm)	Difference, Skin friction Coeff. (%)
1342.5	211854	3.2	-1.298%
1615.3	246574	3.0	4.699%
1613.4	288524	2.8	4.576%
1608.2	344986	2.6	4.239%
1542.8	378692	2.5	0%
1543.1	415743	2.4	0.0194%
1542.7	460938	2.3	-0.00648%

The values of the modelling parameters were established as follows:

- Mesh: In order to obtain the required solution accuracy, the mesh had to be sufficiently fine. The selected five prismatic layers on the walls corresponding to a 378692-element grid-size mesh (see Figure 3.1) provided adequate resolution.
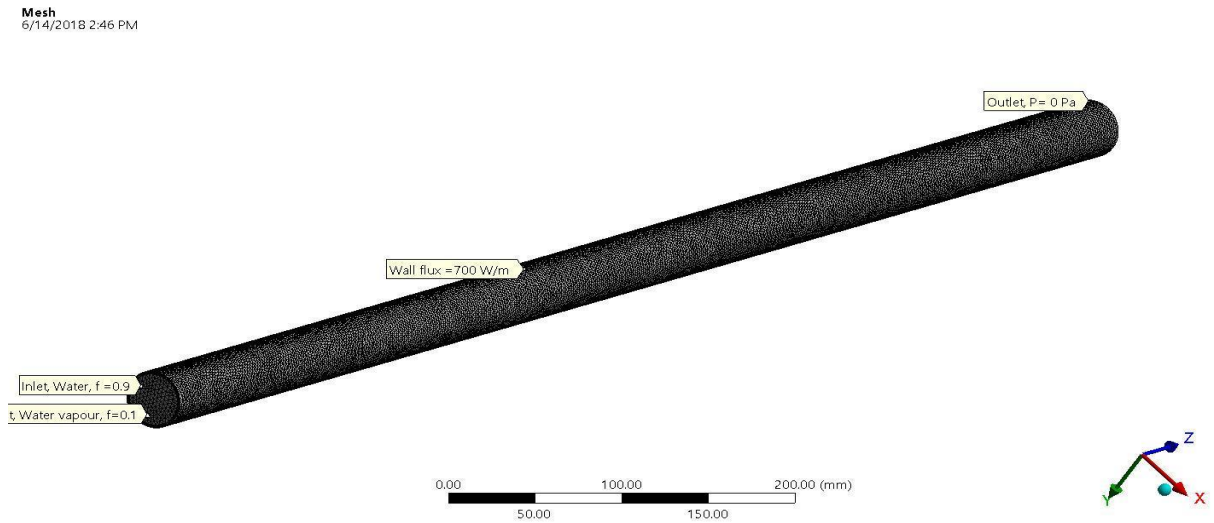

Figure. 3 Mesh of the fluid domain

- Convergence Criterion: Since this study involved transient state flow, it was important to reduce the grid sizes and time-step to be spatially and temporarily convergent. At the 378692 elements convergence had a magnitude of 10^{-9} at 500 iterations in a 2nd order high-resolution scheme. Therefore, to improve the computational times, all simulations were performed at time-steps were 0.001s.

- Boundary Conditions: The Dirichlet and Neumannn mathematical formulations were applied to the inlet and outlet, respectively for the boundary conditions. The inlet conditions of a computational domain typically involved a defined velocity profile ($1/7^{th}$ power law as a User-Defined-Function) and a turbulence intensity of 5%.

Table 2. Modelling parameters

Feature	Description	Details
Mesh	Tetrahedral with prismatic layers	7 prismatic layers
	Elements	378692
	Time-steps	0.001s
Time Dependence	Transient calculations	For flow separation
	Iteration	500

| &Turbulence Modelling	Shear Stress Transport (SST) model with AUTOMATIC near-wall treatment		For two-phase flow seperation
Boundary Conditions	Inlet Boundary	Inlet velocity profile	$1/7^{th}$ power law
		Flow intensity	5%
	Outlet Boundary	Static pressure	0 Pascal
Convergence Criterion	RMS for mass, pressure and velocity residuals		
	High-resolution scheme, 1st order implicit method, Finite Volume method (FVM)		

4. Results and Discussions
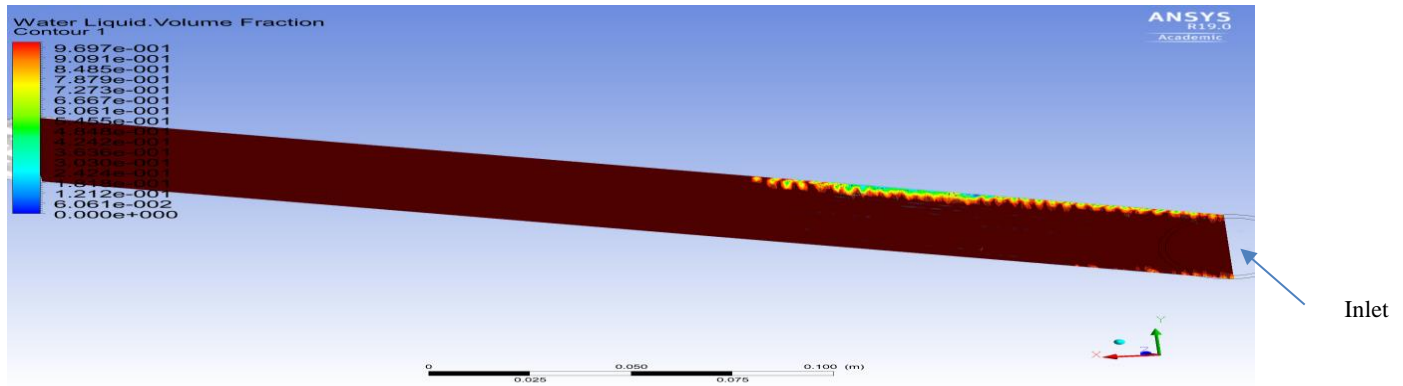
Figure 4. Water-Liquid Volume Fraction at 3m/s

The water-liquid volume fraction at 3 m/s is shown in Figure 4. It clearly indicates the diminishing of the water (liquid) vapor fraction at the upper wall of the domain. It is also good to note that the bulk mass of the fluid at the centerline still contains a high water (liquid) vapor fraction, which indicates that as bubbles are formed more at the domain peripheral, these bubbles move along the wall to reach the upper of the domain, which would be expected as fusion back into the liquid would occur towards the center of the domain, and bubble generation would be high at the walls. Bubbles are also noted entrapped in the bulk flow, moving towards the upper peripheral.
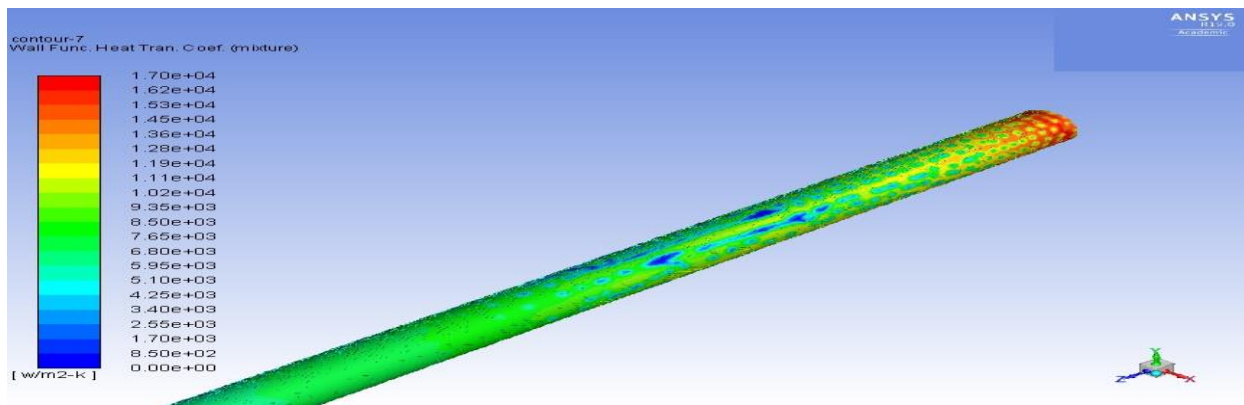

Figure 5. Wall Heat Transfer Coefficient at 3m/s

Figure 5 indicates the wall heat transfer coefficient for 3 m/s simulation. As the nucleate boiling diminishes the heat transfer coefficient starts to decrease until it diminishes completely. Analysis confirmed that when the temperature of the wall increases, the vaporization cores increased, which not only increased the generation rate of vapor, but also accelerated the evaporation, which due to buoyancy resulted in the vapor gathering in the upper section of the tube. The heat transfer in the vapor phase is very low and when the intensity of the heat transfer reduces, the heat transfer coefficient reduces and the temperature of the wall increases.
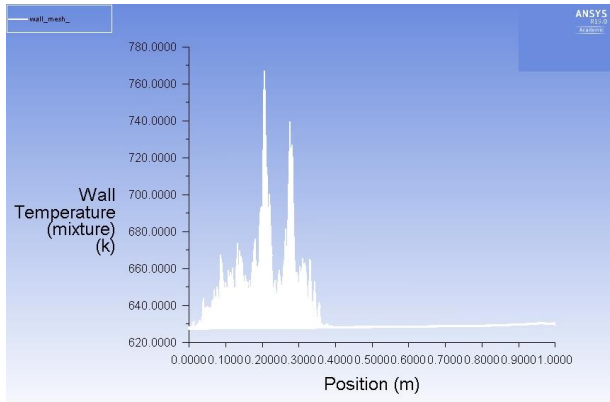
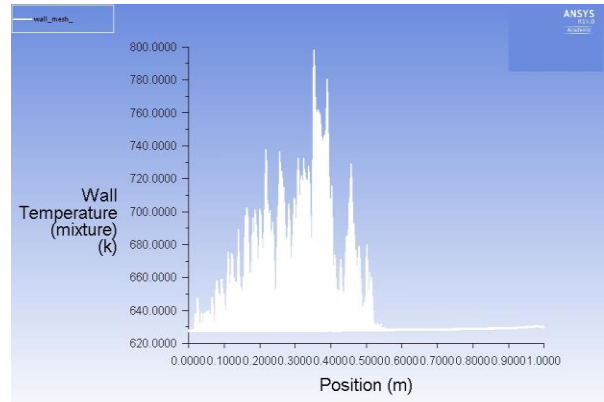Figure 6. Wall Temperature across Domain at 3m/s   Figure 7. Wall Temperature across Domain 5m/s

Figures 6 and 7 show the wall temperature profiles across the domains for the 3m/s and 5m/s simulations. These temperatures are noted due to the decrease in the wall heat transfer coefficients obtained at the upper walls during accumulation of bubbles and dry-out commencement. Note that the onset of complete dry-out is later down the domain flow direction for 5m/s. This is due to the turbulent nature of the increased velocity flow at the upper wall which destroys the dry-out generation and move it further down the domain. At 3m/s the partial dry-out peaks are clearly evident before the sharp complete dry-out peak is reached. With a velocity of 5m/s the partial dry-out peaks are much sharper, and the onset of complete dry-out clearly reaching a higher temperature.
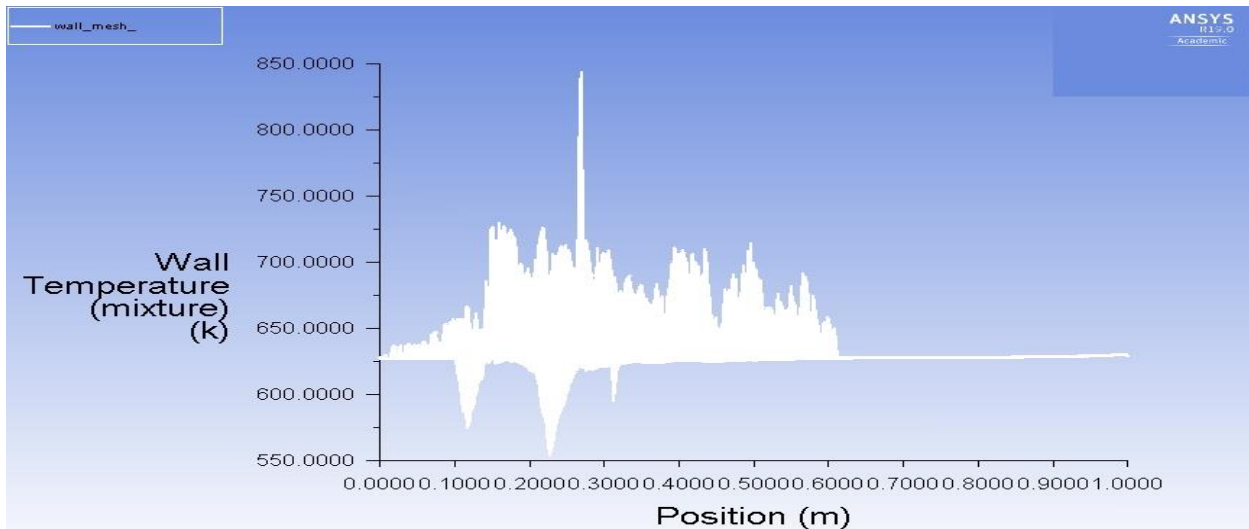

Figure 8. Wall Temperature across Domain at 10m/s

Figure 8 shows the wall temperature profile across the 10m/s domain. From the 10m/s run, a strange yet, understandable phenomena occurs with relation to the increase in wall temperature across the fluid flow domain. There are positions along the domain where the mean temperature around the circumference along the domain has high temperature differences. The lower temperatures are caused by the high fluid velocity stopping the nucleate boiling process from occurring due to turbulences and quickly absorbing the input heat at the bottom of the domain and moving it along the domain flow direction. The bubbles have moved up towards the top and result in sharp temperature

increases at the upper peripheral. There is a sharp spike in temperature, and the position's vapor fraction indicates a small complete dry-out position.

To conserve the boiler tubing and increase the service life thereof, it is obvious that a higher bulk flow velocity would be recommended through the horizontal sections of the boiler tubing. The average wall temperature at the upper wall is much lower than that noted of the 3m/s and 5m/s flow velocities. These tubes are still riser tubes within the furnace, and due to the saturated steam and water separation with the aid of cyclone separators/scrubbers within the steam drum, it is thus only a small portion of the riser tubing bulk mass which would be entering the steam drum at a lower temperature. For the case study boiler, these hanger tubes with horizontal sections above the furnace, account for 3.7% of the total riser volume.

By further material sensitivity analysis, remaining useful life studies were performed. At 943K immediate failure would occur if the tube was new. This is based on the assumption that for the thin tube wall thickness, the mean tube temperature would be very close to the domains wall temperature. At 3m/s, tube failure would occur around 40000 hours. At 5m/s failure would occur at just below 10000 hours. 10m/s flow will result in failure well below 10000 hours operation. All failures occur below the A1 line as per Figure 1, and would thus be categorized as sub-critical Short Term Overheating failures.

5. Conclusion

With an increase in fluid temperature within the flow domain, it is clear that heat transfer increases within the fluid as velocity increases. It would be clear that point of low to no water (liquid) fraction would result in heat not being taken away from the tube wall directly related to the domain position, as water has a higher heat transfer capacity compared to that of water (vapor) with most points being at superheat. With lower heat flux input, longer lengths of tube can be utilized in applications without the risk of short tube life. Analysis is fairly comparable with published literature, and previous works, but would require additional tests at various heat fluxes and velocities to be able to scrutinize critical velocities against certain temperatures. The flow maps noted are similar in nature to that of works published by LiLi et al (2012) and Yu et al (2013) indicating bubble generation moving to the upper wall of the tube, with the bulk mass flow being moved to the bottom of the tube, with a near-perfect turbulent flow regime. This analysis indicates how critical maximum flow velocities have effect on the heat transfer coefficients with a flow domain, with turbulent flow instability having great effect on the material wall temperatures. Horizontal boiler tubing are at higher risk that vertical tubing for steam blanketing/ departure from nucleate boiling, due to the effects of buoyancy on the steam bubble generation. A higher degree of tube temperature and internal flow dynamics is required to ensure safe operation of the boiler tubing. Installation of thermocouples on the horizontal boiler tubing will indicate real-time tube wall temperatures, which in turn would provide data to accurately predict remaining useful life of the tubing during excursions. This can be linked to a master fuel trip, or boiler de-loading logic when or if tube wall temperatures are increasing out of its reliable operating window. This will allow for root cause analysis to be performed for system upsets, without further exposing the tubes to this out-of-design operating temperatures. Tubing should also be fitted with orifices specifically sized to give the most optimal fluid velocities across the wide range of flow requirements for the boiler outputs as required by the turbine. The higher the steam demand at the turbine, the higher the heat input and flow rate requirements within the boiler. Heat input can be drastically optimized to ensure that only the required amount for the steam generation is required. Soot cleaning within the furnace allows for higher heat intake within the lower furnace regions at the vertical walls, which would in turn, reduce the amount of heat the horizontal tubes above the furnace are exposed to. Burner alignment should also be optimized to decrease the likelihood of direct flame impingement on tubing which could reduce the cooling abilities of a specific section of tubing within the flow loop.

References

Emara-Shabaik, H.E., Habib, M.A. and Al-Zaharna, I., 2009. Prediction of risers' tubes temperature in water tube boilers. Applied Mathematical Modelling, 33(3), pp.1323-1336.

Ekambara, K., Sanders, R.S., Nandakumar, K. and Masliyah, J.H., 2008. CFD simulation of bubbly two-phase flow in horizontal pipes. Chemical Engineering Journal, 144(2), pp.277-288.

da Silva Lima, R.J., Quibén, J.M. and Thome, J.R., 2009. Flow boiling in horizontal smooth tubes: New heat transfer results for R-134a at three saturation temperatures. Applied Thermal Engineering, 29(7), pp.1289-1298.

Yu, S., Li, H., Lei, X., Feng, Y., Zhang, Y., He, H. and Wang, T., 2013. Influence of buoyancy on heat transfer to water flowing in horizontal tubes under supercritical pressure. Applied thermal engineering, 59(1-2), pp.380-388.

Bergman, T., Lavine, A., Incropera, F. & Dewitt, D., 2011. Fundamentals of Mass and Heat Transfer. 7th ed. Jefferson City: John Wiley & Sons Inc.

Collier, J. & Thome, J., 1994. Convective Boiling and Condensation. New York: Clarendon Press.

Dooley, R. & McNaughton, W., 2007. Boiler and Heat Recovery Steam Generator Tube Failures: Theory and Practice Volume 2: Water-Touched Tubes. 1st ed. California: Electric Power Research Institute.

Dooley, Boiler and Heat Recovery Steam Generator Tube Failures: Theory and Practice Volume 1: Fundamentals. 1st ed. California: Electric Power Research Institute.

French, D., 1993. Metallurgical Failures in Fossil Fired Boilers. 3rd ed. New York: Wiley.

Kandlikar, S. G., 2010. Scale effects on flow boiling heat transfer in microchannels: A fundamental perspective. International Journal of Thermal Sciences, 49(7), pp. 1073-1085.

Karayiannis, T. G. e. a., 2010. Flow patterns and heat transfer for flow boiling in small to micro diameter tubes. Heat Transfer Engineering, 31(4), pp. 257-275.

Martin, R., 2009. Field Guide: Boiler Tube Failure. 1st ed. Boston, MA: Electric Power Research Institute. 3-5

Thome, J., 2007. Boiling Heat Transfer Inside Plain Tubes. Shawnee Oklahoma: Wolverine Tube Inc. (10), 16.

Tibirica, C. B. a. G. R., 2013. "Flow boiling in micro-scale channels–Synthesized literature review.. International Journal of Refrigeration, 36(2), 301-324.

V. Kefer, W. K. A. W. K., 1988. Critical Heat Flux (Chf) And Post-Chf Heat Transfer In Horizontal And Inclined Evaporator Tubes. International Journal Of Multiphase Flow, 15(3), 385-392.

Iudicello, F, Introduction to computational fluid dynamics and application to internal flow problems. London: IHS-ESDU, 2008, 77

LiLi Gao, Lin Zhang, ZhiLei Ma, Chen Xu, ZhangPing Xiao, MingZhao Du, The Numerical Simulation of Flow and Boiling Heat Transfer of Two Phases in Horizontal Tube, 2012 Asia-Pacific Power and Energy Engineering Conference, 27-29 March 2012

Siriboonluckul, N., Juntasaro, E. & Juntasaro, V, Application of k-SST turbulence model for separated particle-laden flows. Proceedings of the 19th Conference of Mechanical Engineering Network of Thailand, Phuket, 2005, 4-6.

Moss, C.J., Barrien, P. and Walczynski, A., 2000. Life management of refinery furnace tubing. International Journal of Pressure Vessels and Piping, 77(2-3), pp.105-112.

Ennis, T., 2009. Safety in design of thermal fluid heat transfer systems. In Symposium series (Vol. 155, pp. 162-169).

Xueqin, L., Gang, L. and Shangqing, L., 2008, April. The development of the boiler water wall tube inspection. In Electric Utility Deregulation and Restructuring and Power Technologies, 2008. DRPT 2008. Third International Conference on (pp. 2415-2420). IEEE.

Ray, A.K., Tiwari, Y.N. and Chaudhuri, S., 2000. Evaluation of mechanical properties and assessment of residual life of a service-exposed water wall tube. Engineering Failure Analysis, 7(6), pp.393-402.

WEI, L.W., SU, H. and SHEN, L.S., 2008. Study for Accident of Steam Boiler Tube Burst [J]. Pressure Vessel Technology, 3, p.012.

Biographies

Jarryd Eugene Wyngaard is a Master of Technology student at the University of Johannesburg within the Mechanical Engineering Department focusing on Fluid Mechanics and Material Sustainability. He spent many years within the Coal Fired Steam Generation Power industry as a Pressure Parts Engineer within the Boiler Engineering Department, and is now employed as an Asset Integrity and Reliability Engineer within the Oil & Gas, Petrochemical, Mining and Power Generation industries. Jarryd has a keen interest in the reduction of thermal steam generation boiler tube failures, and has dedicated much of his career for the advancement of the reliability and sustainability fields across industries.

Thokozane Kunene is a lecturer in the department of Mechanical Engineering Technology at the University of Johannesburg in South Africa. He has been Project Manager at Automate Industry Development Centre (2009-2017). He holds a Master's degree in Mechanical engineering from Cape Peninsula University of Technology (2017) and a Bachelor degree in Mechanical Engineering from the Tshwane University of Technology (2006). His primary research areas are Fluid Mechanics, Energy Efficiency, Green Technologies and Computational Fluid Dynamics.

Dr Lagouge Tartibu is a senior lecturer in the department of Mechanical Engineering Technology at the University of Johannesburg in South Africa. He has been a Lecturer for Cape Peninsula University of Technology (2007-2012) and Mangosuthu University of Technology (2013-2015). He holds a Doctorate degree in Mechanical engineering from Cape Peninsula University of Technology (2014) and a Bachelor degree in Electromechanical Engineering from the University of Lubumbashi (2006). His primary research areas are thermal science, electricity generation and refrigeration using thermo-acoustic technology, mathematical analysis/optimization and mechanical vibration.